

This article was downloaded by:

On: 16 January 2011

Access details: *Access Details: Free Access*

Publisher *Taylor & Francis*

Informa Ltd Registered in England and Wales Registered Number: 1072954 Registered office: Mortimer House, 37-41 Mortimer Street, London W1T 3JH, UK



Journal of Energetic Materials

Publication details, including instructions for authors and subscription information:

<http://www.informaworld.com/smpp/title~content=t713770432>

Nanoenergetic Composite of Mesoporous Iron Oxide and Aluminum Nanoparticles

Bhushan Mehendale^a; Rajesh Shende^a; Senthil Subramanian^a; Shubhra Gangopadhyay^a; Paul Redner^b; Deepak Kapoor^b; Steven Nicolich^b

^a Department of Electrical and Computer Engineering, University of Missouri, Columbia, MO ^b US Army ARDEC, Picatinny Arsenal, NJ

To cite this Article Mehendale, Bhushan , Shende, Rajesh , Subramanian, Senthil , Gangopadhyay, Shubhra , Redner, Paul , Kapoor, Deepak and Nicolich, Steven(2006) 'Nanoenergetic Composite of Mesoporous Iron Oxide and Aluminum Nanoparticles', *Journal of Energetic Materials*, 24: 4, 341 – 360

To link to this Article: DOI: 10.1080/07370650600896715

URL: <http://dx.doi.org/10.1080/07370650600896715>

PLEASE SCROLL DOWN FOR ARTICLE

Full terms and conditions of use: <http://www.informaworld.com/terms-and-conditions-of-access.pdf>

This article may be used for research, teaching and private study purposes. Any substantial or systematic reproduction, re-distribution, re-selling, loan or sub-licensing, systematic supply or distribution in any form to anyone is expressly forbidden.

The publisher does not give any warranty express or implied or make any representation that the contents will be complete or accurate or up to date. The accuracy of any instructions, formulae and drug doses should be independently verified with primary sources. The publisher shall not be liable for any loss, actions, claims, proceedings, demand or costs or damages whatsoever or howsoever caused arising directly or indirectly in connection with or arising out of the use of this material.

Nanoenergetic Composite of Mesoporous Iron Oxide and Aluminum Nanoparticles

BHUSHAN MEHENDE
RAJESH SHENDE
SENTHIL SUBRAMANIAN
SHUBHRA GANGOPADHYAY

Department of Electrical and Computer Engineering,
University of Missouri, Columbia, MO

PAUL REDNER
DEEPAK KAPOOR
STEVEN NICOLICH

US Army ARDEC, Picatinny Arsenal, NJ

Ordered mesoporous Fe₂O₃ was synthesized using cetyltrimethylammonium chloride (CTAC) and polyethylene glycol octadecyl ether (Brij 76) surfactant templates. The gel time was monitored as a function of the concentration ratio of precursor to the surfactant. As-prepared FeOOH gels were extracted in ethanol to remove the surfactant and calcined at 200–400°C for 6 h so that α -Fe₂O₃ is produced. The FTIR spectra of these gels reveal complete removal of surfactant and water impurities and the presence of Fe-O vibrations. TEM images show ordering of mesopores in the gels prepared using surfactant templating and no ordering of the pores in the gels prepared without surfactant. The gels after calcinations were mixed

Address correspondence to Shubhra Gangopadhyay, Department of Electrical and Computer Engineering, University of Missouri, 243 EBW, crossing of 6th Street and Stewart Ave, Columbia, MO 65211. E-mail: gangopadhyays@missouri.edu

with aluminum nanoparticles to prepare nanoenergetic composites. The burn rate of the nanocomposites containing ordered mesoporous Fe₂O₃ mixed with Al nanoparticles was compared with the one containing Fe₂O₃ with no ordering of mesopores and Al nanoparticles.

Keywords: al-nanoparticles, burn rate, ordered mesoporous Fe₂O₃, surfactant templating

Introduction

Nanoenergetic composites containing oxidizer and fuel nanoparticles are of increasing interest due to very high burning rates reported in the literature. Typically, for nanoenergetic composites consisting of non-porous solid oxidizers and fuels, the rates of combustion are limited by a heat transfer conduction mechanism, whereas with porous materials, the energy transfer rates rely on a convective mechanism of heat transfer [1] which is reported [1–3] to produce much higher burning rates (Mesoporous materials have poresizes in the range of 2–50 nm providing a huge surface area). Mesoporous materials have pores in the range of 20–500 Å in diameter provide a huge surface area. Therefore, nanoenergetic material prepared using this material may achieve still higher burn rates. Mesoporous Fe₂O₃ has other applications such as in catalysis [4], as magnetic materials [5], electrochemical capacitor [6], and biosensors [7].

Porous oxidizer can be easily prepared using the sol-gel approach. In general, this process involves the formation of a solid phase, the sol, which consists of a colloidal suspension containing solid particles of a diameter of a few hundred nanometers suspended in a liquid phase. The gelation of the same produces a new phase (the gel) by condensation or polymerization of the particles to generate a solid macromolecule immersed in a liquid phase (solvent). Removal of the liquid phase results in a porous solid matrix. The sols are randomly distributed in a solution, which, on polymerization, produce randomly oriented pores with various sizes. Physical processes such as stirring and sonication can improve dispersion of sols in a solution, but they have limitations. When an oxidizer with randomly oriented pores is

combined with a fuel, a lower interfacial contact area is anticipated. However, as self-propagating reactions of oxidizer and fuel are diffusionally controlled, higher interfacial area between fuel and oxidizer is desired to achieve higher hot spot density of the combustion wave front and higher reaction propagation velocity [2]. To achieve higher interfacial area, it is therefore important to combine an oxidizer with ordered porous structure and fuel nanoparticles with narrow size distribution. This will improve the performance of the nanoenergetic composite.

To achieve ordered arrangement of pores and uniform pore size distribution, surfactant templating method is very effective. Surfactant micelles self-assemble in a solution and produce a template with uniform micelles distribution. When inorganic oxidizer precursor is introduced in a solution, it goes around the micelles template. Removal of the template leaves behind the imprints of an inorganic oxidizer network with pores in place of micelles. Therefore, by using a surfactant templating method, an oxidizer with ordered pore distribution and uniform pore sizes can be easily achieved. Recently, synthesis of mesoporous Fe_2O_3 using a surfactant templating method was reported [8–10]. The other methods of interests to prepare mesoporous Fe_2O_3 could be aerogel route, aero-sol-gel synthesis, etc. In aerogel route for the synthesis of Fe_2O_3 , the gel was prepared using normal sol gel method and subjected to the supercritical fluid [11,12]. The role of supercritical fluid was to extract solvent from the gel, leaving the pores behind. Aero-sol-gel synthesis of mesoporous Fe_2O_3 particles involved the addition of precursor directly into a gas phase followed by gas phase polymerization or condensation [1].

In the synthesis of mesoporous Fe_2O_3 , precursors such as Fe (III)-ethoxide [8,13], $FeCl_3$ [1,5,14], etc. have been used by researchers. Among these, Fe (III)-ethoxide was used with a surfactant templating of cetyltrimethylammonium bromide (CTAB). In this method, a precipitate was obtained instead of gel, which on solvent extraction and calcination yielded a microstructure with nonuniform distribution of pores of 3–5 nm [8]. The calcination process is one of heating the finely ground material at high temperatures to remove the chemically bound water and/or surfactant. The same precursor was used to synthesize

hexagonal ordered mesoporous Fe_2O_3 (pore size 5.4 nm) [13] using ligand-assisted liquid crystal templating method [15]. In the method using FeCl_3 precursor, propylene oxide or epichlorohydrin was used as a proton scavenger to achieve mesoporous Fe_2O_3 with 2–3 nm pores. However, no ordering of the pores was observed in the microstructure reported for aerosol-gel synthesis of mesoporous Fe_2O_3 particles [1]. Recently, we also reported sol-gel synthesis of $\alpha\text{-Fe}_2\text{O}_3$ from Fe(III)-nitrate precursor using propylene oxide as proton scavenger [16].

When mesoporous Fe_2O_3 (lower density) was mixed with Al nanoparticles, it performed better as compared to a homogeneous mixture of Fe_2O_3 and Al nanoparticles in terms of its energetic properties [2,17]. In this article, we report synthesis of nanoenergetic composite of mesoporous Fe_2O_3 and Al nanoparticles. Mesoporous Fe_2O_3 was synthesized using a micelles template-assisted sol-gel synthesis route using two surfactants. In one approach, we use cationic cetyltrimethylammonium chloride (CTAC), and non-ionic co-polymer, Brij 76, in the other. It is known that the addition of surfactant during sol-gel synthesis will bring ordering of the pores. The burn rate of nanoenergetic composite containing ordered mesoporous Fe_2O_3 with Al nanoparticles was compared with the one containing mesoporous Fe_2O_3 with no ordering of the pores and Al nanoparticles.

Experimental

Synthesis of FeOOH Gel without Surfactant

To synthesize FeOOH gel, 1.0 g of iron nitrate ($\text{Fe}(\text{NO}_3)_3 \cdot 9\text{H}_2\text{O}$) was dissolved in 8.5 mL of ethanol, and to this 5.2 mL of propylene oxide (Sigma Aldrich, St. Louis, MO) was added under constant stirring. The gel time for this mixture was around 16 h.

Synthesis of FeOOH Using CTAC as the Templating Agent

One gram of ($\text{Fe}(\text{NO}_3)_3 \cdot 9\text{H}_2\text{O}$) was dissolved in 8.5 mL of ethanol and 0.4 mL surfactant ($\text{C}_{19}\text{H}_{42}\text{NCl}$, Arquad 16/29) solution (17% by weight) was then added. The resultant mixture was sonicated

for 10 min to ensure complete dissolution of iron nitrate and homogenous mixing of the surfactant in the solution. To this, 5.2 mL of the propylene oxide was added slowly under constant stirring. The gelling time for this was less than 1 min. For low surfactant concentration of 3 wt%, the gel time was 2–3 min, and for the gels prepared with no surfactant the gel time was about 16 h (see Table 1).

Synthesis Using Brij 76 as the Templating Agent

Polyethylene glycol octadecyl ether (Brij 76) was obtained from Sigma Aldrich and was used without purification. In a beaker, 17% (w/v) solution of Brij 76 was prepared in ethanol and was heated to 60°C and maintained for 15 min under constant stirring. The latter was labeled as solution A. In another beaker, 1.0 g of Fe(NO₃)₃·9H₂O was dissolved in 5.5 mL of ethanol. This solution was designated as solution B. The solution B was placed in a sonicator bath for about 10 min to ensure complete dissolution of iron nitrate in ethanol. Solution B was slowly added to solution A under gentle stirring. The resultant solution mixture was then placed in sonication bath for another 10 min. After sonication, 5.2 mL of the propylene oxide was added to this solution under gentle stirring. The gel time was around 1–2 min. Various concentrations of precursor, surfactant, and their gel time are listed in Table 1.

Surfactant Template Removal Using Ethanol Extraction and Calcination

As-prepared FeOOH gels were soaked in excess ethanol for 2 days at the temperature of 60°C under magnetic stirring to remove the surfactant template. The gels were then filtered and calcined at 200°C for 6 h. Few FeOOH gel samples were calcined directly at 200–400°C for 6 h.

Characterization

Gels prepared under various experimental conditions (see Table 1) were characterized using Thermo Nicolet FTIR (Fourier transform infrared) spectrophotometer. To prepare samples for FTIR analysis, the gels were dispersed in 2-propanol for

Table 1
Effect of concentration of precursor, solvent, surfactant, and propylene oxide on the gel time

Serial number	Iron nitrate (gm)	Ethanol (mL)	Propylene oxide (mL)	Surfactant	Surfactant volume, mL (wt%)	Gelling time (hr)
1	1.0	8.5	5.2	None	—	16
2	1.0	15.0	10.2	None	—	22
3	1.0	8.5	5.2	None	—	12
4	2.5	8.6	2.5	None	—	3
5	2.0	3.3	0.8	None	—	1.3
6	4.0	13.8	5.0	None	—	3.4
7	1.0	8.5	5.2	CTAC	0.4 (3%)	0.050
8	1.0	8.5	5.2	CTAC	1.13 (8.5%)	0.016
9	1.0	8.5	5.2	CTAC	2.2 (17%)	<0.016
10	1.0	8.5	5.2	Brij 76	0.4 (3%)	0.059
11	1.0	8.5	5.2	Brij 76	1.13 (8.5%)	0.017
12	1.0	8.5	5.2	Brij 76	2.2 (17%)	0.016

5 min, spin-coated on a silicon wafer, and dried at 90°C for 10 min. The samples were characterized using the total number of scans of 1024 with resolution of 8 cm⁻¹. All the FTIR spectra were corrected for the substrate absorption and for their baseline using a 20-point baseline correction using the Microcal Origin 6.0 software. The samples were also characterized using transmission electron microscopy (TEM), JEOL 1200 EX, to understand their microstructures, especially ordering of the mesopores.

Mixing of Mesoporous Fe₂O₃ and Al-Nanoparticles

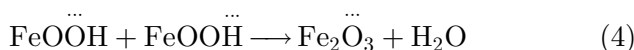
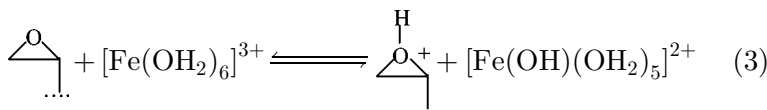
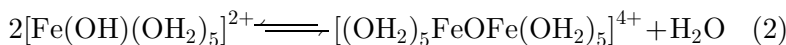
Accurately weighed 0.2 g of mesoporous iron oxide and 0.12 g of Al particles (80 nm from Nanotechnology Inc. Austin, TX) were placed in 2-propanol in a sealed bottle and the mixture was sonicated in an ultrasonic bath for 6–8 h.

Burn Rate Measurement

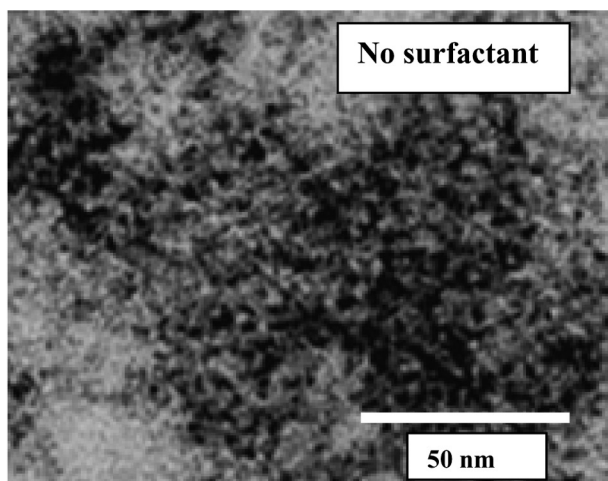
The burn rate or combustion wave speed of the composite of mesoporous Fe₂O₃ and aluminum nanoparticles was measured using on-chip diagnostic technique [18] and by the optical method [2] in a confined arrangement. The on-chip method is based on time-varying resistance (TVR) of sputter-coated thin platinum film, in which the resistance of the film changes as energetic reaction propagates over it. By knowing the voltage differential over a time period and the length of a TVR film, the burn rate velocity was determined. For the optical method, a Lexane tube of 0.8 cm³ volume was filled up with the nanoenergetics powder and inserted into an aluminum block. This block was mounted with the holders for the optical fibers. The ends of the tube were confined against the bricks inside an environmental metallic enclosure. Tektronix TDS460A 4-channel digital oscilloscope was fitted to a set of spatially spaced ThorLabs photodiodes and optical fibers. The energetic reaction was triggered with a spark igniter at one end of the tube and the oscilloscope recorded an output voltage signal in time for the sequentially placed photo detectors. The burn rate of energetic material was then calculated on the basis of the differential between signal rise times of the individual photo detector.

Results and Discussion

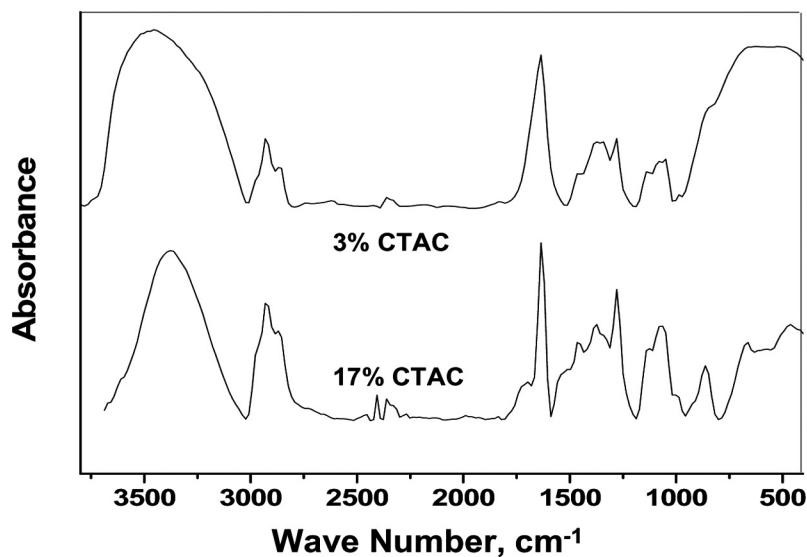
In the reaction route chosen, $\text{Fe(III)(NO}_3)_3 \cdot 9\text{H}_2\text{O}$ produced $[\text{Fe}(\text{OH}_2)_6]^{3+}$ complex in presence of $\text{C}_2\text{H}_5\text{OH}$ with the liberation of water molecules and the $(\text{NO}_3)^-$ species. $[\text{Fe}(\text{H}_2\text{O})_6]^{3+}$ species (hexa aquairon (III) ion) are highly unstable and undergo reversible reaction with water to produce dimer (reaction 2) [19,20]. The added propylene oxide scavenges protons (reaction 3), which upon further hydrolysis produce $\alpha\text{-FeOOH}$ (ferrihydrite). When two FeOOH molecules combine, $\alpha\text{-Fe}_2\text{O}_3$ is generated with the liberation of a water molecule [14]. Overall reaction sequence for the hydrolysis of Fe(III) ion and proton scavenging action of propylene oxide are summarized below.



The time required for FeOOH gelation to take place at various concentration ratios of $\text{Fe(III)(NO}_3)_3 \cdot 9\text{H}_2\text{O}$, $\text{C}_2\text{H}_5\text{OH}$ and propylene oxide is given in Table 1. We notice that, at the volume ratio 2:3.3:0.8 of $\text{Fe(III)(NO}_3)_3 \cdot 9\text{H}_2\text{O}:\text{C}_2\text{H}_5\text{OH}:\text{propylene oxide}$, the time required for gelation was 1.3 h, whereas for 1:8.5:5.2 the gelation could occur after 16 h. This suggests that if ethanol volume is in excess, hydrated Fe -complex requires higher volume of propylene oxide for proton scavenging action, resulting in longer gelation time. FeOOH gels were annealed at 400°C for 3 h in a Thermolyne box furnace. After calcination, FeOOH is converted into Fe_2O_3 . TEM image of Fe_2O_3 sample presented in Fig. 1a shows that the pores are randomly distributed and at some points pore boundaries are collapsed. We observe that the pore size varies between 2 and 10 nm. Furthermore, TEM image shows nonuniformity of porous gel over the whole area.



(a)



(b)

Figure 1. (a) TEM image of Fe_2O_3 gel prepared without using the surfactants and calcined at 400°C for 6 h; (b) FTIR spectra of as-prepared Fe_2O_3 gel prepared using 3 and 17% CTAC surfactant.

The time required for FeOOH gel formation with respect to various surfactant concentrations is given in Table 1 and FTIR spectra of as-prepared FeOOH gels using 3 and 17% CTAC templating are shown in Fig. 1b. It is seen that the time required for gel formation decreased from 3 min to less than a minute as surfactant concentration increased from 3 to 17%. In the FTIR spectra, the presence of $-\text{CH}$ vibrations at around 2930 cm^{-1} suggests organic impurities and broad stretching vibration of $-\text{OH}$ peak around $3000\text{--}3600\text{ cm}^{-1}$ implies the presence of the water in the sample in the form of free and bonded water. The peak at around 1630 cm^{-1} is the bending mode of the water in the sample. The absorption peaks around 800 to 1500 cm^{-1} are associated with the solvent ($\text{C}_2\text{H}_5\text{OH}$) used, residual propylene oxide or by-products of the ring opening reaction of propylene oxide. The broad absorption peak around $500\text{--}700\text{ cm}^{-1}$ can be associated with the Fe-O linkages.

Cetyltrimethylammonium chloride (CTAC, cationic surfactant) interacts with hydrated Fe species through S^+I^- type of interactions, where S represents a surfactant or the organic species and I^- represents the Fe species, mainly oxyhydroxides/oxides. The surfactant micelle in solution develops δ -positive charge on its head due to the chlorine atoms and the hydrocarbon tail. Thus, positive charge on the methyl group of this surfactant gets attracted toward the negative charge of oxygen present in FeOOH upon surfactant addition, which could be attributed to S^+I^- type of interactions.

FeOOH gels prepared using 17% CTAC concentration were calcined at $200\text{--}400^\circ\text{C}$ for 6 h. The FTIR spectra of as-prepared gels as shown in Fig. 2 indicate broad water peak around $3000\text{--}3600\text{ cm}^{-1}$, the organic peak at around 2939, 800, and 1500 cm^{-1} , and the amorphous Fe_2O_3 peaks from 480 to 520 cm^{-1} . This indicates that these gels have free and bonded water and the organics presumably are trapped inside the gel pores. However, the reduction in water and organic peaks were observed when the gel was annealed at 200°C for 6 h. After annealing FeOOH gels at 300°C , the $-\text{CH}$ peak at 2939 cm^{-1} (due to the surfactant) was almost absent, indicating that the major portion of the surfactant was removed; however, the

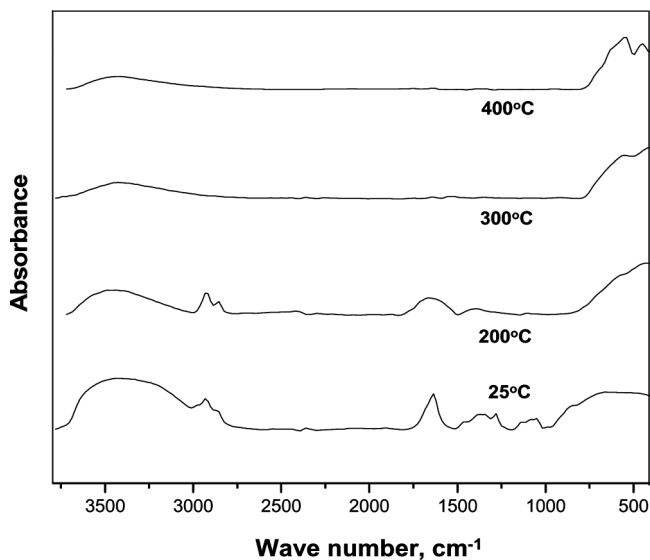


Figure 2. FTIR spectra of Fe_2O_3 gel prepared using 17% CTAC surfactant and calcined at various temperatures of 200–400°C for 6 h.

water peak was still prominent. It is to be noted that the increase in sharpness of peaks at around 500 cm^{-1} suggests crystallization of Fe_2O_3 from amorphous phase. The FTIR spectra for the gel calcined at 400°C for 6 h shows complete removal of the organics; however, a small water peak can be accounted for as incomplete conversion of FeOOH into Fe_2O_3 .

A TEM image of FeOOH gel prepared using CTAC templating agent and calcined at 400°C for 6 h is shown in Fig. 3. The pore size is around 3–4 nm, which is consistent with those reported for Fe_2O_3 using CTAB (cetyltrimethylammonium bromide) surfactant [8]. Small pore size could be due to the shorter length of the hydrocarbon chain in the compound ($\text{C}_{19}\text{H}_{42}\text{NCl}$), which determines size of the micelles and thus the size of pores. As CATC concentration was increased from 3 to 17%, more ordering of the mesopores was noticed. Also, the pore size distribution was found to be lower for the gels

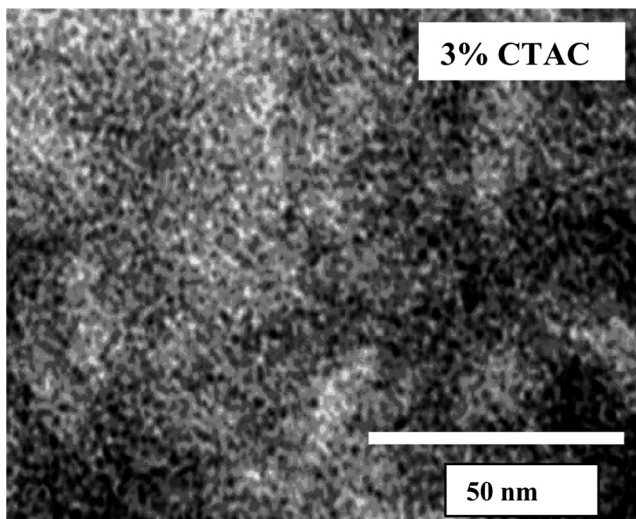


Figure 3. TEM images of porous Fe₂O₃ prepared by templating method using 3% surfactant.

prepared with 17% CTAC as compared with 3% CTAC or no surfactant (Fig. 1a).

Pore size can be increased if larger micelles are employed. Therefore, FeOOH gels were prepared using Brij 76 (co-block polymer) surfactant templating. This non-ionic surfactant interacts with hydrated Fe species via hydrogen bonding, which is normally represented as (S^o I^o). As the concentration of Brij 76 increased from 3 to 17%, time required for gel formation reduced from 3 min to about a minute (Table 1). The FTIR spectra of FeOOH gels prepared using 17% surfactant concentration and calcined at 200–400°C for 6 h are presented in Fig. 4. The –CH peak was present for the gels calcined at 300°C, which was not the case with those prepared using CTAC and calcined at the same temperature. One of the reasons could be that the long hydrocarbon chain in Brij 76 might require high temperature and longer time as compared with CTAC. FeOOH gels calcined at 400°C for 6 h did not show organic impurities but did show very prominent crystalline peaks of Fe₂O₃.

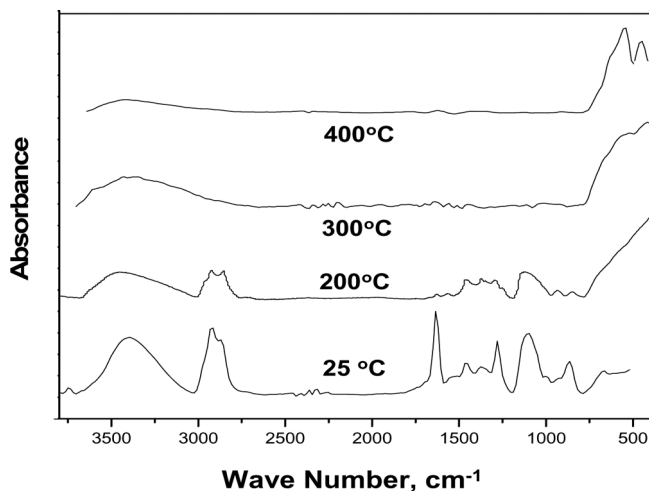


Figure 4. FTIR spectra of FeOOH gels prepared using Brij 76 surfactant and calcined at 200–400°C for 6 h.

One of the problems encountered during calcination is densification, which can reduce overall porosity. Accelerated thermal ramp rates can further worsen this problem. This can be solved by subjecting FeOOH gels to solvent extraction or supercritical CO_2 treatment. Development in the synthesis of ordered structure silicates like MCM-41 (mesoporous crystalline material with hexagonal one-dimensional pores) have made use of the chemical route in extraction of the templating agents while preserving the pore walls. It is believed that the polar solvents like ethanol [8,13], chloroform [21], acidic solution of dimethyl ether [22], etc., can dissolve the organic species and still preserve the pore boundaries intact. The organic species once dissolved remain in the solution and are removed easily by filtration. In our method, FeOOH gels prepared using Brij 76 template were extracted using ethanol as per the procedure outlined in the Experimental section. The gels were characterized by FTIR to measure peak intensity of organic and water-based impurities. It is observed that the solvent extraction reduces the ratio of surfactant to iron oxide by 89%, while the ratio of water to iron oxide is reduced by

78%. After extracting with ethanol, gels were calcined at 200°C for 6 h with the ramp rate of 1°C/min. The TEM image shown in Fig. 5a indicates homogeneous distribution of the pores with

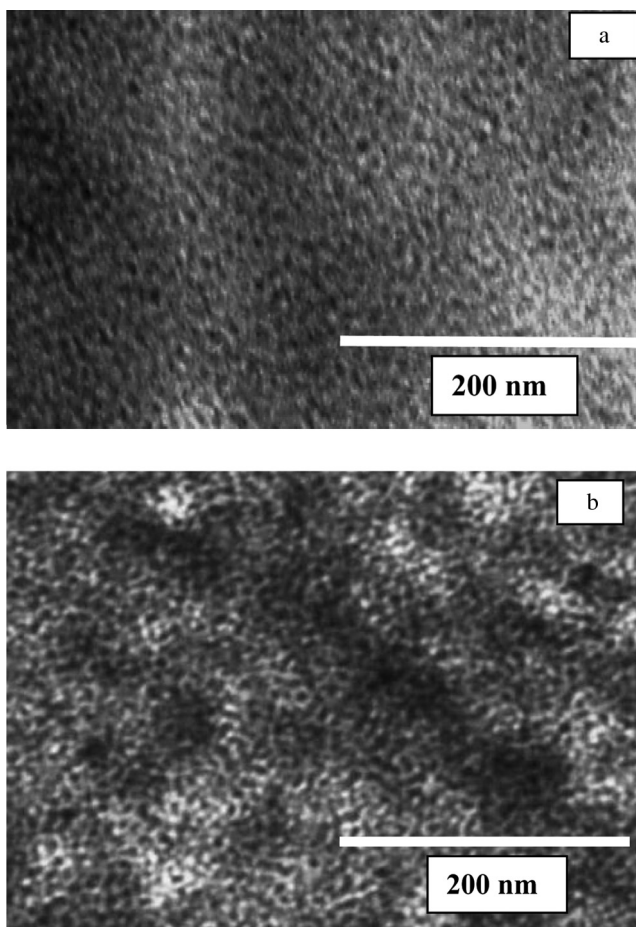


Figure 5. (a) TEM image of Fe₂O₃ prepared using Brij 76 after ethanol extraction followed by calcination at 200°C for 6 h; (b) TEM of Fe₂O₃ prepared using Brij 76 templating, supercritical CO₂ extraction (80°C, 7000 psi), followed by calcination at 400°C for 3 h.

an average pore size of about 8–10 nm. This pore size is approximately double the pore size obtained using CTAC templating. Few gel samples were subjected to supercritical CO₂ extraction at 80°C, 7000 psi for 24 h and later calcined at 400°C for 3 h. The TEM image of this gel sample is presented in Fig. 5b, which shows a highly porous structure. However, higher processing cost and secondary phase formation during isenthalpic expansion of supercritical fluids can make this process less attractive for producing porous oxidizer on a large scale.

Energetic composites were prepared using ordered mesoporous Fe₂O₃, which was synthesized as per the procedure outlined in the Experimental section. It is expected that the ordering of mesopores should yield higher propagation rates of energetic reaction. Mesoporous Fe₂O₃ prepared using 17% Brij 76 template was mixed with aluminum nanoparticles (80 nm) (see Experimental section) and the burn rate of composite was measured using on-chip diagnostic method [18]. The equivalence ratio [2], Φ , which is defined as

$$\Phi = \frac{(\text{fuel/oxidizer})_{\text{actual}}}{(\text{fuel/oxidizer})_{\text{stoichiometry}}} \quad (5)$$

was varied between 0.6 and 1.6. The effect of equivalence ratio on the burn rate in open environment is shown in Fig. 6. It is observed that the burn rate is optimum at around equivalence ratio of 1.4.

Mesoporous iron oxide was prepared using surfactant concentrations in the range of 3 to 20% by weight. This was mixed with Al nanoparticles at the optimum equivalence ratio of 1.4 and the burn rate of composite was measured. Figure 7 shows the effect of Brij 76 concentration used to prepare iron oxide on the burn rates of the composites. The burn rates of the composites containing Fe₂O₃ prepared using the surfactant was found to be significantly higher than those prepared using no surfactant. At the surfactant concentration of 3 to 20%, the change in the burn rate was not significant. There is a possibility that residual contaminants can reduce the burn rate at higher surfactant concentration.

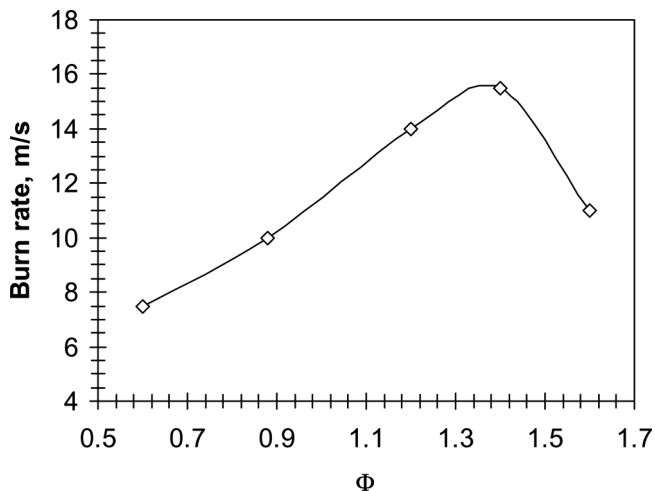


Figure 6. Burn rates of mesoporous Fe_2O_3 prepared using Brij 76 templating and mixed with Al nanoparticles (80 nm size) as a function of equivalence ratio (Φ).

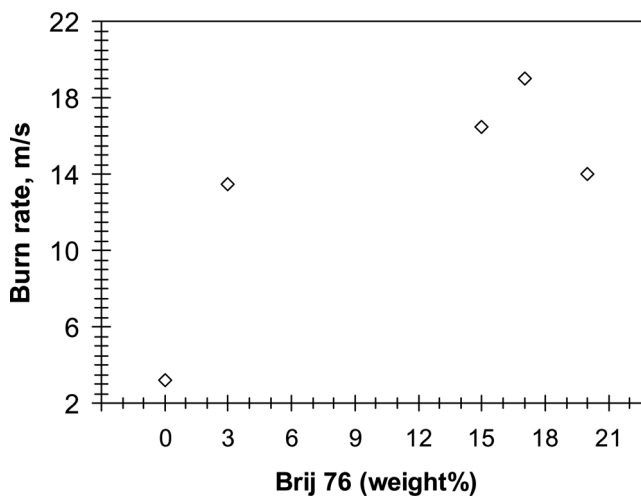


Figure 7. Burn rate as a function of composite of Fe_2O_3 and Al nanoparticles, where Fe_2O_3 was prepared using various surfactant concentrations.

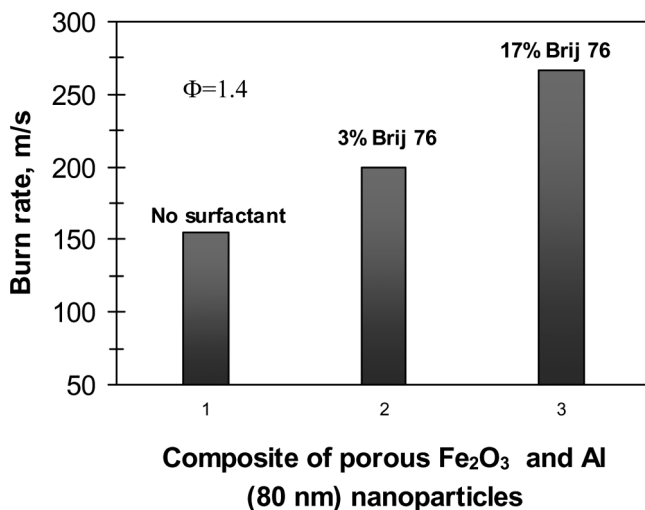


Figure 8. Comparison of the confined burn rates of composite of ordered mesoporous $\text{Fe}_2\text{O}_3/\text{Al}$ nanoparticles with the composite of Fe_2O_3 (no ordering of pores)/Al nanoparticles.

In Fig. 8, we compared confined burn rates of various composites obtained by the optical method (see Experimental section). The burn rates of the composites in a confined arrangement were found to be higher than in an open burn arrangement, which is consistent with those reported by others [2]. Composites of ordered mesoporous Fe_2O_3 and Al nanoparticles were found to have higher burn rates than the one containing iron oxide with no ordering of mesopores and Al nanoparticles. The use of surfactant increases ordering of the mesopores due to self-assembly of micelles and decreases the pore size distribution in an oxidizer. When this oxidizer is mixed with the fuel nanoparticles and ignited, the hot spot density in the combustion wavefront will increase leading to higher burn rates.

Conclusions

Ordered mesoporous Fe_2O_3 oxidizer was synthesized using a surfactant templating method. Using CTAC templating

the pore size was 3–4 nm, whereas the pore size increased to 8–10 nm for Brij 76 templating. With surfactant templating, not only narrow pore size distribution was attained but pores were also homogeneously distributed throughout the sample matrix. The burn rate of the nanocomposites containing ordered mesoporous Fe_2O_3 mixed with Al nanoparticles was higher than those prepared using Fe_2O_3 with no ordering of mesopores. The improvement in the burn rate can be attributed to the ordered arrangement of mesopores in closest proximity to the Al nanoparticles. This is believed to enhance interfacial contact area between oxidizer and fuel for a thermite reaction.

Acknowledgement

The authors gratefully acknowledge the financial support by the U.S. Army, ARDEC, Picatinny, NJ, and the National Science Foundation. The authors are thankful to the reviewers for their excellent comments.

References

- [1] Prakash, A., A. V. McCormic, and M. R. Zachariah. 2004. Aerosol-gel synthesis of nanoporous iron oxide particles: A potential oxidizer for nanoenergetic materials. *Chemistry of Materials*, 16: 1466.
- [2] Plantier, K. B., M. L. Pantoya, and A. E. Gash. 2005. Combustion wave speeds of nanocomposites Al/ Fe_2O_3 : The effects of Fe_2O_3 particles synthesis technique. *Combustion and Flame*, 140: 299.
- [3] Son, S., J. Busse, B. Asay, P. Paterson, J. Mang, B. Bockmon, and M. Pantoya. 2002. Propagation studies of Metastable Intermolecular Composite (MIC). *Proceedings of the International Pyrotechnics Society, the Twenty-Ninth International Pyrotechnics Seminar*, Colorado, July 14–19, 203.
- [4] Li, P., D. E. Miser, S. Rabiei, R. T. Yadav, and M. R. Hajaligol. 2003. The removal of carbon monoxide by iron oxide nanoparticles. *Applied Catalysis B: Environmental*, 43: 151.
- [5] Long, J. W., M. S. Logan, C. P. Rhodes, E. E. Carpenter, R. M. Stroud, and D. R. Rolinson. 2004. Nanocrystalline iron oxide aerogels as mesoporous magnetic architectures. *Journal of the American Chemical Society*, 126: 16879.

- [6] Wu, N. L., S. Y. Wang, C. Y. Han, D. S. Wu, and L. R. Shiue. 2003. Electrochemical Capacitor of Magnetite in Aqueous Electrolytes. *Journal of Power Sources*, 113: 173.
- [7] Cosnier, S., A. Senillou, M. Gratzel, P. Comte, N. Vlachopoulos, N. J. Renault, and C. Mortelet. 1999. A glucose biosensor based on enzyme entrapment within polypyrrole films electrodeposited on mesoporous titanium dioxide. *Journal of Electroanalytical Chemistry*, 469: 176.
- [8] Srivastava, D. N., N. Perkas, A. Gedanken, and I. Felner. 2002. Sonochemical synthesis of mesoporous iron oxide and accounts of its magnetic and catalytic properties. *The Journal of Physical Chemistry B*, 106: 1878.
- [9] Lezau, A., M. Trudeau, G. M. Tsoi, L. E. Wenger, and D. J. Antonelli. 2004. Mesostructured Fe-oxide synthesized by ligand-assisted templating with a chelating triol surfactant. *The Journal of Physical Chemistry B*, 108: 5211.
- [10] Yuan, Z.-Y., T.-Z. Ren, and B.-L. Su. 2004. Surfactant mediated nanoparticle assembly of catalytic mesoporous crystalline iron oxide materials. *Catalysis Today*, 93–95: 743.
- [11] Fricke, J. and A. Emmerling. 1998. Aerogels—recent progress in production techniques and novel applications. *Journal of Sol-Gel Science and Technology*, 13: 299.
- [12] Gash, A. E., J. H. Satcher, and R. L. Simpson. 2003. Strong akaganeite aerogel monoliths using epoxides: synthesis and characterization. *Chemistry of Materials*, 15: 3268.
- [13] Jiao, F. and P. G. Bruce. 2004. Two- and Three-dimensional mesoporous iron oxides with microporous walls. 2004. *Angewandte Chemie International Edition* 43: 5958.
- [14] Gash, A. E., T. M. Tillotson, J. H. Satcher, Jr., J. F. Poco, L. W. Hrubesh, and R. L. Simpson. 2001. Use of epoxides in the sol-gel synthesis of porous iron(III) oxide monoliths from Fe(III) Salts. *Chemistry of Materials*, 13: 999.
- [15] Antonelli, D. M., A. Nakahira, and J. Y. Ying. 1996. Ligand assisted liquid crystal templating in mesoporous niobium oxide molecular sieves. *Inorganic Chemistry*, 35: 3126.
- [16] Talantsev, E. F., M. L. Pantoya, C. Camagong, B. Lahlouh, S. M. Nicolich, and S. Gangopadhyay. 2005. Ferrihydrite gels derived in the $\text{Fe}(\text{NO}_3)_3 \cdot 9\text{H}_2\text{O} - \text{C}_2\text{H}_5\text{OH} - \text{CH}_3\text{CHCH}_2\text{O}$ Ternary System. *Journal of Non-Crystalline Solids*, 351: 1426.
- [17] Mehendale, B. 2005. *Synthesis of Ordered Nanoporous Composites*. M.S. Thesis, University of Missouri—Columbia.

- [18] Bhattacharya, S., Y. Gao, S. Apperson, S. Subramaniam, E. Talantsev, R. V. Shende, and S. Gangopadhyay. 2006. A novel on-chip diagnosis method to detect flame velocity of nanoscale thermites. *Journal Energetic Materials*, 24: 1.
- [19] Knight, R. J. and R. N. Sylva. 1974. Precipitation in hydrolysed iron(III) solutions. *Journal of Inorganic and Nuclear Chemistry*, 36: 591.
- [20] Dousma J. and P. L. Bruyn. 1976. Hydrolysis-precipitation studies of iron solutions. I. Model for hydrolysis and precipitation from Fe(III) nitrate solutions. *Journal of Colloid and Interface Science*, 56: 527.
- [21] Khramov, A. N. and M. M. Collinson. 2001. Sol-Gel preparation of mesoporous silica films by templating with polystyrene microspheres. *Chemical Communications*, 8: 767.
- [22] Zhao, X. S., G. Q. Max, and C. Song. 2003. Immobilization of aluminum chloride on MCM-41 as a new catalyst for ligand-phase isopropylation of naphthalene. *Journal of Molecular Catalysis A: Chemical*, 191: 67.